

## Direct recording and molecular identification of the calcium channel of primary cilia

Paul G. DeCaen<sup>1,\*</sup>, Markus Delling<sup>1,\*</sup>, Thuy N. Vien<sup>2</sup>, and David E. Clapham<sup>1,3,†</sup>

<sup>1</sup>Howard Hughes Medical Institute, Department of Cardiology, Children's Hospital Boston, 320 Longwood Avenue, Boston, MA 02115, USA

<sup>2</sup>Department of Neuroscience, School of Medicine, Tufts University, Boston, MA 02111, USA

<sup>3</sup>Department of Neurobiology, Harvard Medical School, Boston, MA 02115, USA

### Summary

A primary cilium is a solitary slender non-motile protuberance of structured microtubules (9+0) enclosed by plasma membrane<sup>1</sup>. Housing components of the cell division apparatus between cell divisions, they also serve as specialized compartments for calcium signaling<sup>2</sup> and Hedgehog (Hh) signaling pathways<sup>3</sup>. Specialized sensory cilia such as retinal photoreceptors and olfactory cilia employ diverse ion channels<sup>4-7</sup>. An ion current has been measured from primary cilia of kidney cells<sup>8</sup> but the responsible genes have not been identified. The polycystin proteins (PC, PKD), identified in linkage studies of polycystic kidney disease<sup>9</sup>, are candidate channels divided into two structural classes: 11-transmembrane (TM) proteins (PKD1, PKD1-L1 and PKD1-L2) remarkable for a large extracellular N-terminus of putative cell adhesion domains and a GPCR proteolytic site, and the 6-TM channel proteins (PKD2, PKD2-L1, PKD2-L2; TRPPs). Evidence suggests that the PKD1s associate with the PKD2s via coiled-coil domains<sup>10-12</sup>. Here, we employ a transgenic mouse in which only cilia express a fluorophore and employ it to directly record from primary cilia and demonstrate that PKD1-L1 and PKD2-L1 form ion channels at high densities in several cell types. In conjunction with the companion manuscript<sup>2</sup>, we show that the PKD1-L1/PKD2-L1 heteromeric channel establishes the cilia as a unique calcium compartment within cells that modulates established Hedgehog pathways.

---

Patch clamp of primary cilia is challenging due to their small dimensions ( $\approx 0.2\text{-}0.5\ \mu\text{m}$  in width,  $1\text{-}12\ \mu\text{m}$  in length), making them difficult to identify *in vivo*. Employing a human retina pigmented epithelium cell line stably expressing the cilia-specific EGFP-tagged

---

Users may view, print, copy, download and text and data- mine the content in such documents, for the purposes of academic research, subject always to the full Conditions of use: [http://www.nature.com/authors/editorial\\_policies/license.html#terms](http://www.nature.com/authors/editorial_policies/license.html#terms)

<sup>†</sup>Correspondence and requests for materials should be addressed to D.E.C. ([dclapham@enders.tch.harvard.edu](mailto:dclapham@enders.tch.harvard.edu)).

\*These authors contributed equally to this work

**Author Information.** Reprints and permissions information is available at [www.nature.com/reprints](http://www.nature.com/reprints).

**Online Content.** Any additional Methods, Extended Data display items and Source Data are available in the online version of the paper; references unique to these sections appear only in the online paper.

**Author Contributions.** All authors designed and conducted experiments and wrote the manuscript.

The authors declare no competing financial interests.

Readers are welcome to comment on the online version of the paper.

*Smoothed* gene (hRPE Smo-EGFP), the cilia could be visualized under confocal fluorescence microscopy and recorded using the method we describe here, whole-cilia patch clamp (Fig. 1a, Extended Data Fig. 1a and Supplementary Video 1). After establishing  $>16$  G $\Omega$  seals and rupturing the cilia membrane, we recorded a surprisingly large, outwardly-rectifying, non-inactivating current ( $I_{\text{cilia}}$ ). Importantly,  $I_{\text{cilia}}$  was recorded from cilia attached or detached from the cell body (Fig. 1b, c and Supplementary Video 2). Current density measured in the detached cilia patch was 56-fold higher than that measured from the hRPE cell body (Methods). These measurements indicate that the primary cilium is partly insulated from the cell body by the structures at the cell-cilia junction (Extended Data Fig. 1a). The outwardly rectifying current was cation-nonspecific (Fig. 1d) with relative permeabilities of  $\text{Ca}^{2+} \approx \text{Ba}^{2+} > \text{Na}^+ \approx \text{K}^+ > \text{NMDG}$  (Extended Data Fig. 1b).

Consistent with the whole-cilia currents, single channel amplitudes were outwardly rectifying (Fig. 1e) and mean open times substantially longer at more depolarized potentials. Extracellular uridine and adenosine phosphates (UDP, ADP, ATP) activated the ciliary current in perforated-cilia recordings, while the non-selective antagonists  $\text{Gd}^{3+}$  and ruthenium red blocked it (Extended Data Fig. 1c-e). Several cell-permeable calmodulin antagonists also activated the conductance. Based on the dimensions of the cilia, we estimate the average membrane surface area to be  $\sim 6.3 \mu\text{m}^2$  ( $\sim 0.063$  pF). Assuming the entire outward rectifying current is carried by the 96 pS conductance, we estimate the primary cilia channel density to be  $29 \pm 2$  channels/ $\mu\text{m}^2$ , similar to endogenous channel densities calculated from excitable tissue plasma membranes and larger than those found in intracellular compartments (Fig. 1f). Thus, the primary cilium is richly populated with  $\text{Ca}^{2+}$ -permeant, relatively nonspecific cation channels that enable a much higher dynamic range of ciliary  $[\text{Ca}^{2+}]$  compared to the cytoplasm.

We generated a transgenic mouse expressing the cilia-specific *Arl13B* gene C-terminally tagged with EGFP (*Arl13B-EGFP<sup>tg</sup>* mouse)<sup>2</sup> and isolated primary cells from mouse RPE (mRPE) and embryonic fibroblasts (MEFs). Primary cilia currents from these primary cells were outwardly rectifying with the same conductance and pharmacological properties as observed in the cilia from the human RPE cell line (Fig. 2; Extended Data Fig. 2). In addition,  $I_{\text{cilia}}$  was observed in the cilia of a human kidney-derived inner medullary collecting duct cell line (IMCD stably expressing *Arl-EGFP*; Fig. 2c, Extended Data Fig. 2d). Ciliary single channel conductances were identical in all 4 cell types (Fig 2e), and activated by extracellular ATP and blocked by  $\text{Gd}^{3+}$  in perforated patch recordings. ATP addition to the bath significantly increased the probability of channel opening ( $P_o$ ) and mean open times (5-7 fold, Fig. 2f, Extended Data Fig. 2e). Since these were in the 'on-cilia' patch configuration (bath-applied ATP), we reasoned that ATP binds a G-protein coupled purinergic receptor to initiate activation of the channels in the patch. Thus,  $I_{\text{cilia}}$  is a common feature of many cell types.

Analysis of hRPE transcripts confirmed expression of several purported ciliary channels<sup>13-16</sup> including *Tmc7*, *TRPV4*, and *PKD1*, *PKD2*, *PKD1-L1* and *PKD2-L1* (Extended Data Fig. 3a). Only siRNAs specific for *PKD1-L1* and *PKD2-L1* reduced both inward and outward currents (Extended Data Fig. 3c-d). These results suggest that  $I_{\text{cilia}}$  is conducted by either *PKD1-L1* or *PKD2-L1* independently, or together as a heteromeric ion channel. To verify

$I_{\text{Cilia}}$  channel proteins, we patch clamped cilia of homozygous PKD2-L1 knockout (*PKD2-L1*<sup>-/-</sup>) crossed with *Arl13B-EGFP* mice. The much-reduced *PKD2-L1*<sup>-/-</sup> MEF ciliary current was linear and failed to activate when stimulated by calmidazolium (Fig. 3b, c). These data establish that PKD2-L1 is a component of  $I_{\text{Cilia}}$ .

Immunoprecipitation of Flag- or HA-tagged PKD1-L1 and PKD2-L1 demonstrated that PKD1-L1 and PKD2-L1 interact (Extended Data Fig. 4a). In whole-cell patch clamp of HEK-293 cells transiently transfected with members of the PKD family, only PKD2-L1 produced a measurable outward current in the plasma membrane (Extended Data Fig. 4b). Together, these data suggest that PKD2-L1, but not PKD1-L1, can form homomeric channels. Based on an alignment of the PKD2 family of proteins (Extended Data Fig. 4c), a cluster of conserved acidic residues in the putative selectivity filter<sup>17</sup> was mutated. Neutralizing two of three extracellular glutamates (E523 and E525, but not E530) to serine or alanine abolished the current (Extended Data Fig. 4b). The homomeric PKD2-L1 channel produced an outwardly rectifying, cationic whole-cell current with a large moderately  $\text{Ca}^{2+}$ -selective conductance (Fig. 4a; Extended Data Fig. 4d). Our results differ from the presumed PKD2-L1 expressed in oocytes<sup>18</sup>: PKD2-L1 currents in our HEK293T cells were outwardly rectifying and not activated by extracellular calcium. The unitary conductance ( $198 \pm 3$  pS) and rectification ratio of homomeric PKD2-L1 is too large to underlie the primary ciliary conductance (compare Fig. 1e and 4d). However, coexpression of the PKD1-L1 and PKD2-L1 yielded a less rectifying whole-cell current with a single channel outward conductance of  $103 \pm 3$  pS (Fig. 4b-d), consistent with that found in RPE primary cilia. In addition, heterologously expressed PKD2-L1 and PKD1-L1 channels were activated by calmodulin antagonists and blocked by  $\text{Gd}^{3+}$  and ruthenium red. Unlike the ciliary current, the heterologously expressed channels were not activated by extracellular uridine and purine analogues (UDP, ADP, ATP; data not shown) suggesting that the receptor/signal transduction pathway in cilia is absent in the whole-cell HEK-293 conditions. These data establish that  $I_{\text{Cilia}}$  is conducted by a heteromer of PKD1-L1 and PKD2-L1 subunits.

Primary cilia have been proposed to sense flow by mechanical activation of the putative PKD1/PKD2 channel<sup>16,19</sup>. Using pressure clamp<sup>20</sup>, we observed no difference in single channel activity at pressures of 0-60 mm Hg (8 kPa) for PKD1-L1/PKD2-L1 in mRPE primary cilia or in heterologous expression (Extended Data Fig. 5). Although channel activity measurably increased at high pressure (80-100 mm Hg; 11-13 kPa), the PKD1-L1/PKD2-L1 channel lacks the sensitivity found in designated mechanosensitive channels<sup>21,22</sup>.

Many members of the TRP superfamily are highly temperature-sensitive<sup>7,23-25</sup> and primary cilia are proposed to be temperature sensors via activation of a thermosensitive  $\text{Ca}^{2+}$  influx<sup>26</sup>. We tested the effect of increasing temperature (22-37°C) on primary cilia and PKD1-L1/PKD2-L1-transfected cells and observed an increase in the  $\text{Gd}^{3+}$ -sensitive current (Extended Data Fig. 6 a, b). When rapidly increasing the bath temperature ( $2.1 \pm 0.2^\circ\text{C/s}$ ), we observed biphasic current activation in the current from RPE primary cilia (from 24-32°C,  $Q_{10} = 6$ ) and heterologously expressed PKD1-L1/PKD2-L1 cilia (from 24-32°C,  $Q_{10} = 8$ ; Extended Data Fig. 6 c). This sensitivity is moderate in comparison to highly temperature-sensitive channels, such as TRPV1-TRPV4 ( $Q_{10} > 20$ ). In any case, temperature gradients are likely inconsequential over the length of cilia and cilia to cytoplasm.

Delling and DeCaen et al<sup>2</sup>. demonstrated that cilia are a specialized calcium compartment, regulated by PKD1-L1 and PKD2-L1 channels, and that they in turn regulate ciliary Smoothed signaling and *Gli* transcription. Here we have demonstrated that PKD1-L1 and PKD2-L1, heteromultimerize to form a calcium-permeant ciliary channel which can be indirectly activated by purines. Future experiments will determine the purine receptor and downstream effectors activating  $I_{\text{Cilia}}$ . Since the PKD1-L1/PKD2-L1 complex is calcium-permeant, but is also inactivated at high internal  $[\text{Ca}^{2+}]$ , we propose that the channel regulates the high resting ciliary calcium level<sup>2</sup>. We hypothesize that these signals modify regulation of Smoothed target genes, in particular *Gli* transcription of genes regulating cell division and growth.

## Methods

### Electrophysiology

hRPE1 Smo-EGFP cells were serum starved 24-72 h prior to electrophysiological recording in order to slow cell growth and induce ciliogenesis. Primary cells cultured from the *Arll3B-EGFP<sup>tg</sup>* mouse tissues (MEF and mRPE) were cultured for less than two passages before they were patch clamped. Data were collected using an Axopatch 200B patch clamp amplifier, Digidata 1440A, and pClamp 10 software. For temperature-controlled experiments, the perfusate was heated using a Warner TC-344B heater controller and in-line heater/cooler while bath temperature was monitored using a thermistor placed in close proximity to the recording electrode. For pressure clamp experiments, membrane pressure was applied using a HSPC-1 high-speed pressure system (ALA Scientific) controlled by pClamp software. Whole-cell and excised inside-out patch currents were digitized at 25 kHz and low pass filtered at 10 kHz. The permeability of monovalent cations relative to that of  $\text{Na}^+$  was estimated from the shift in reversal potential on replacing external  $\text{Na}^+$  bath solution (150 mM X, 10 mM HEPES, 0.5 mM  $\text{CaCl}_2$ , pH 7.4), where X was NaCl, NaMES, KCl, BaCl<sub>2</sub>, CaCl<sub>2</sub>, or NMDG. Permeability ratios were calculated as:

$$P_X = P_{\text{Na}} [\text{Na}^+]_{\text{out}} / [X]_{\text{out}} = \{ \exp((F/RT)(V_{\text{rev}} - V_m)) \}$$

where  $[X]_{\text{out}}$  is defined as the extracellular concentration of the given ion, P is defined as the permeability of the ion indicated by the subscript, F is Faraday's constant, R is the gas constant, T is absolute temperature and  $V_{\text{rev}}$  is the reversal potential for the relevant ion.

**Estimates of cilia channels per membrane surface area**—The number of channels per cilia was calculated as  $N = I / P_o(i)$ , where N = number of channels; I is the whole-cilium current at +100 mV;  $P_o$  is the open probability (calculated at +100 mV from ~1 s-long traces), and  $i$  is the single channel amplitude at +100 mV. Based in the slope of the single channel records from RPE cilia, the channel conductance,  $\gamma = 80 \pm 3$  pS inward and  $\gamma = 96 \pm 3$  pS outward. RPE cilia channel mean open time at -100 mV and 100 mV were  $0.22 \pm 0.02$  and  $14 \pm 3$  ms, respectively. For simplification we represent the cilia as a cylinder and thus its surface area is given by  $A = 2\pi r(r+h)$  where h is the height (5  $\mu\text{m}$  on average) and radius (r) varies from 0.15 to 0.25  $\mu\text{m}$  as measured in electron micrographs. Assuming  $r = 0.2 \mu\text{m}$ ,

then the surface area is  $\sim 6.3 \mu\text{m}^2$  and capacitance ( $C_m$ , assuming  $1 \mu\text{F}/\text{cm}^2$ ) = 0.063 pF (for comparison, surface areas of typical cells are  $\sim 2000 \mu\text{m}^2$  with  $C_m = 20$  pF). Current density measured in the detached cilia patch and the hRPE cell body was  $1730 \pm 98$  pA/pF and  $31 \pm 4$  pA/pF respectively. The equivalent circuit of the whole-cilia recording assumes that the resistance between cilia and cell is sufficiently high to neglect the contributions from the cell, since cilia ripped from the cell and sealed over show essentially the same result as cilia attached to the cell.

## Molecular Biology and Biochemistry

**Plasmids and heterologous expression of PKD channels**—HEK 293T cells were transfected using Lipofectamine 2000 (Invitrogen) reagent. hPKD2, hPKD2-L1 and hPKD2-L2 cDNAs were obtained from Open Biosystems and a Hemagglutinin (HA) Tag was added to the N-terminus using PCR. The resulting cDNAs were subcloned into an IRES enhanced green fluorescence protein (EGFP)-containing vector. hPKD1-L1 cDNA was synthesized (Bio Basic, Amherst NY) with a Flag-Tag at the C-terminus. hPKD1L1, hPKD1 and hPKD1-L2 were subcloned into an IRES red fluorescence protein (RFP)-containing vector. Transfected cells cultured at  $37^\circ\text{C}$  and plated onto glass coverslips and were recorded 24-48 h later. For the co-transfected cells in Figure 4, the cDNA was transfected at a 5:1 ratio for PKD1-L1 and 2L-1. Whole-cell patches for recordings from the cell body were obtained using electrodes of 1.5-2.5 M $\Omega$  and excised inside-out patches were obtained using pipettes of 5-7 M $\Omega$  resistances. Saline conditions are the same as those used for primary cilia.

**Inhibition and Detection of Transcripts**—Smo-EGFP expressing hRPE1 cells were transfected with 50 pM of siRNA and 5  $\mu\text{l}$  RNAiMAX (Life Technologies) in a 3.5 cm dish. Cells were seeded at 230,000 cells/plate. 60 h after transfection, cells were serum-starved and cilia recordings performed 48 h after serum starvation. hRPE1 cells in a 3.5 cm dish were washed  $\times 1$  with PBS and lysed in 1 ml TRIZOL for RNA extraction according to the manufacturer's instructions. RNA was reverse transcribed using the QuantiTect reverse transcription kit (Qiagen). Gene specific primers were designed using Primerbank (<http://pga.mgh.harvard.edu/primerbank/>). Gene specific products were amplified by PCR and gene expression was visualized by agarose gel electrophoresis.

**Immunoprecipitation**—HEK 293T cells were transfected in a 10 cm dish with the indicated combinations of PKD1-L1 Flag and PKD2-L1-HA using Lipofectamine according to the manufacturer's instructions (Life Technologies). 24 h after transfection cells were lysed in 2 ml RIPA buffer (20 mM Tris-HCl; pH 7.5, 150 mM NaCl, 1 mM EDTA, 1% NP-40 and 1% sodium deoxycholate and protease inhibitors added (Complete, Roche). After centrifugation at 15,000 g for 10 min at  $40^\circ\text{C}$ , 1.5 ml of the supernatant was added to 30  $\mu\text{l}$  Anti-Flag M2 Agarose (Sigma-Aldrich) and incubated overnight at  $40^\circ\text{C}$ . Agarose beads were spun down at 1000 g for 5 min and washed  $\times 5$  with RIPA buffer. The agarose beads were resuspended in LDS samples buffer containing 2%  $\beta$ -mercaptoethanol, heated at  $75^\circ\text{C}$  for 5 min, and proteins were separated on a 4%-12% BisTris gel. After transfer to PVDF membrane, blots were probed with anti-Flag (Sigma Aldrich) or anti-HA (Roche) antibodies.

## Supplementary Material

Refer to Web version on PubMed Central for supplementary material.

## Acknowledgments

Paul DeCaen was supported by NIH T32 HL007572. Animal work was, in part, supported by NIH P30 HD18655 to the IDDRC of Boston Children's Hospital. We thank Betsy Navarro, Nat Blair, Julia Doerner, Sebastien Febvay, and the members of the Clapham laboratory for valuable advice and assistance.

## References

1. Bornens M. The centrosome in cells and organisms. *Science*. 2012; 335:422–426. [PubMed: 22282802]
2. Delling M, DeCaen PG, et al. Primary cilia are specialized calcium signaling organelles. *Nature*.
3. Corbit KC, et al. Vertebrate Smoothed functions at the primary cilium. *Nature*. 2005; 437:1018–1021.10.1038/nature04117 [PubMed: 16136078]
4. Hardie RC, Minke B. The *trp* gene is essential for a light-activated Ca<sup>2+</sup> channel in *Drosophila* photoreceptors. *Neuron*. 1992; 8:643–651. [PubMed: 1314617]
5. Shin JB, et al. *Xenopus* TRPN1 (NOMPC) localizes to microtubule-based cilia in epithelial cells, including inner-ear hair cells. *Proc Natl Acad Sci U S A*. 2005; 102:12572–12577.10.1073/pnas.0502403102 [PubMed: 16116094]
6. Stortkuhl KF, Hovemann BT, Carlson JR. Olfactory adaptation depends on the Trp Ca<sup>2+</sup> channel in *Drosophila*. *The Journal of neuroscience : the official journal of the Society for Neuroscience*. 1999; 19:4839–4846. [PubMed: 10366618]
7. Story GM, et al. ANKTM1, a TRP-like channel expressed in nociceptive neurons, is activated by cold temperatures. *Cell*. 2003; 112:819–829. [PubMed: 12654248]
8. Kleene NK, Kleene SJ. A method for measuring electrical signals in a primary cilium. *Cilia*. 2012; 1
9. Arnaout MA. Molecular genetics and pathogenesis of autosomal dominant polycystic kidney disease. *Annu Rev Med*. 2001; 52:93–123. [PubMed: 11160770]
10. Celic A, Petri ET, Demeler B, Ehrlich BE, Boggon TJ. Domain mapping of the polycystin-2 C-terminal tail using de novo molecular modeling and biophysical analysis. *J Biol Chem*. 2008; 283:28305–28312. [PubMed: 18694932]
11. Yu Y, et al. Structural and molecular basis of the assembly of the TRPP2/PKD1 complex. *Proc Natl Acad Sci U S A*. 2009; 106:11558–11563. [PubMed: 19556541]
12. Zhu J, et al. Structural model of the TRPP2/PKD1 C-terminal coiled-coil complex produced by a combined computational and experimental approach. *Proc Natl Acad Sci U S A*. 2011; 108:10133–10138. [PubMed: 21642537]
13. Gherman A, Davis EE, Katsanis N. The ciliary proteome database: an integrated community resource for the genetic and functional dissection of cilia. *Nat Genet*. 2006; 38:961–962.10.1038/ng0906-961 [PubMed: 16940995]
14. Andrade YN, et al. TRPV4 channel is involved in the coupling of fluid viscosity changes to epithelial ciliary activity. *J Cell Biol*. 2005; 168:869–874. [PubMed: 15753126]
15. Raychowdhury MK, et al. Characterization of single channel currents from primary cilia of renal epithelial cells. *J Biol Chem*. 2005; 280:34718–34722. [PubMed: 16079132]
16. Yoshida S, et al. Cilia at the node of mouse embryos sense fluid flow for left-right determination via Pkd2. *Science*. 2012; 338:226–231. [PubMed: 22983710]
17. Hille, B. *Ion Channels of Excitable Membranes*. 3rd. Sinauer Associates Inc; 2001.
18. Chen XZ, et al. Polycystin-L is a calcium-regulated cation channel permeable to calcium ions. *Nature*. 1999; 401:383–386. [PubMed: 10517637]
19. Praetorius HA, Spring KR. A physiological view of the primary cilium. *Annu Rev Physiol*. 2005; 67:515–529. [PubMed: 15709968]

20. Besch SR, Suchyna T, Sachs F. High-speed pressure clamp. *Pflugers Archiv : European journal of physiology*. 2002; 445:161–166.10.1007/s00424-002-0903-0 [PubMed: 12397401]
21. Coste B, et al. Piezo proteins are pore-forming subunits of mechanically activated channels. *Nature*. 2012; 483:176–181.10.1038/nature10812 [PubMed: 22343900]
22. Sukharev SI, Blount P, Martinac B, Blattner FR, Kung C. A large-conductance mechanosensitive channel in *E. coli* encoded by *mscL* alone. *Nature*. 1994; 368:265–268.10.1038/368265a0 [PubMed: 7511799]
23. Xu H, et al. TRPV3 is a calcium-permeable temperature-sensitive cation channel. *Nature*. 2002; 418:181–186.10.1038/nature00882 [PubMed: 12077604]
24. Benham CD, Gunthorpe MJ, Davis JB. TRPV channels as temperature sensors. *Cell calcium*. 2003; 33:479–487. [PubMed: 12765693]
25. Voets T, et al. The principle of temperature-dependent gating in cold- and heat-sensitive TRP channels. *Nature*. 2004; 430:748–754.10.1038/nature02732 [PubMed: 15306801]
26. Kottgen M, et al. TRPP2 and TRPV4 form a polymodal sensory channel complex. *J Cell Biol*. 2008; 182:437–447. [PubMed: 18695040]
27. Cang C, et al. mTOR Regulates Lysosomal ATP-Sensitive Two-Pore Na(+) Channels to Adapt to Metabolic State. *Cell*. 201310.1016/j.cell.2013.01.023
28. Fieni F, Lee SB, Jan YN, Kirichok Y. Activity of the mitochondrial calcium uniporter varies greatly between tissues. *Nature communications*. 2012; 3:1317.10.1038/ncomms2325
29. Shenkel S, Sigworth FJ. Patch recordings from the electrocytes of *Electrophorus electricus*. Na currents and PNa/PK variability. *The Journal of general physiology*. 1991; 97:1013–1041. [PubMed: 1650809]
30. Brisson A, Unwin PN. Quaternary structure of the acetylcholine receptor. *Nature*. 1985; 315:474–477. [PubMed: 4000275]

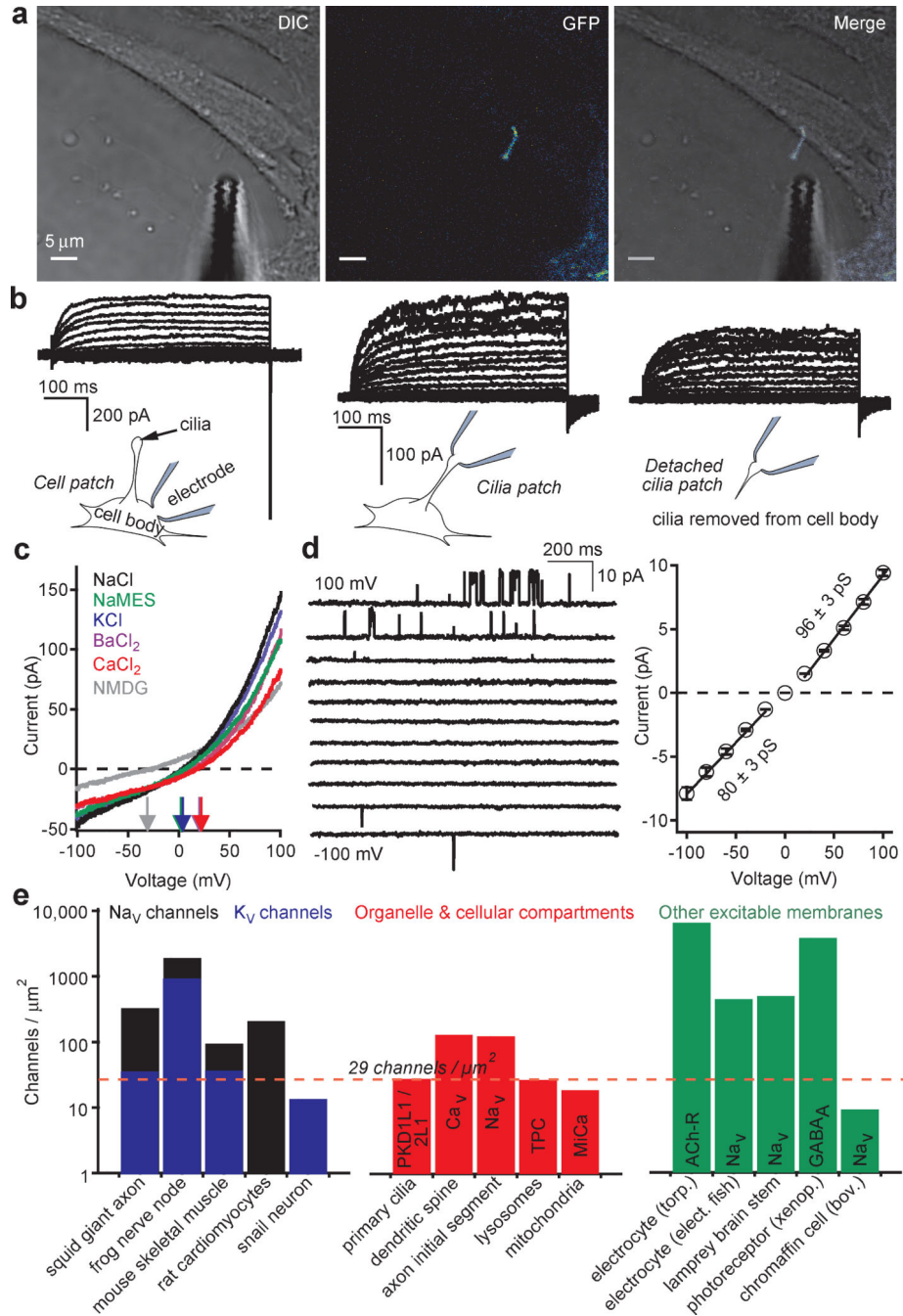


### Figure 1. A calcium-selective ion channel is richly expressed in primary cilia

(a) Confocal image of an hRPE Smo-EGFP cell and patch clamp electrode. (b) Whole-cell leak-subtracted currents elicited by 1 s depolarizing pulses from -100 to 100 mV in +5 mV increments recorded from the cell body, primary cilia and an excised primary cilium (recorded from the same cilium). (c) Whole-cell currents activated by ramp voltage protocols from -100 to +100 mV measured from the primary cilia where extracellular Na<sup>+</sup>-based saline was replaced by the cation indicated. (d) Single channel currents activated by 1.5 s depolarizations to the indicated potentials (left) and average current amplitudes (right;  $\pm$



SEM, n = 8 cilia). (e) Estimated endogenous cilia ion channel densities compared to those from other biological preparations<sup>17,27-30</sup>.

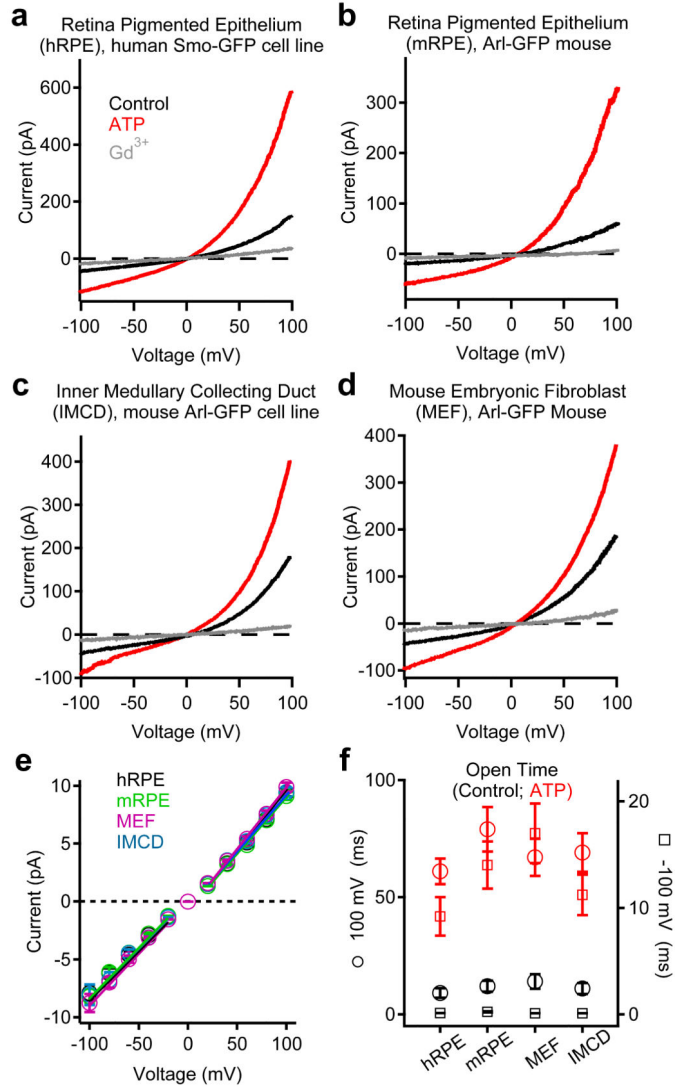


**Figure 2. Primary cilia currents measured from four different cell types**

Averaged cilia current traces in control and bath-applied 100  $\mu\text{M}$  ATP or 10  $\mu\text{M}$  Gd<sup>3+</sup> from: (a) human RPE cell line stably expressing Smoothened-EGFP; (b) Primary mRPE cells from the Arl13B-EGFP<sup>tg</sup> mouse; (c) Kidney IMCD cell line stably expressing Arl-EGFP and (d) Primary embryonic fibroblasts from the Arl13B-EGFP<sup>tg</sup> mouse. (e) Average single channel current/voltage relation. The slope is used to estimate conductance ( $\pm$  SEM,  $n = 4-7$  cilia). (f) Average open times in the presence and absence of ATP at -100 and +100 mV potentials measured from the cilia of RPE Smo-EGFP cells ( $\pm$  SEM,  $n = 6$  cilia).

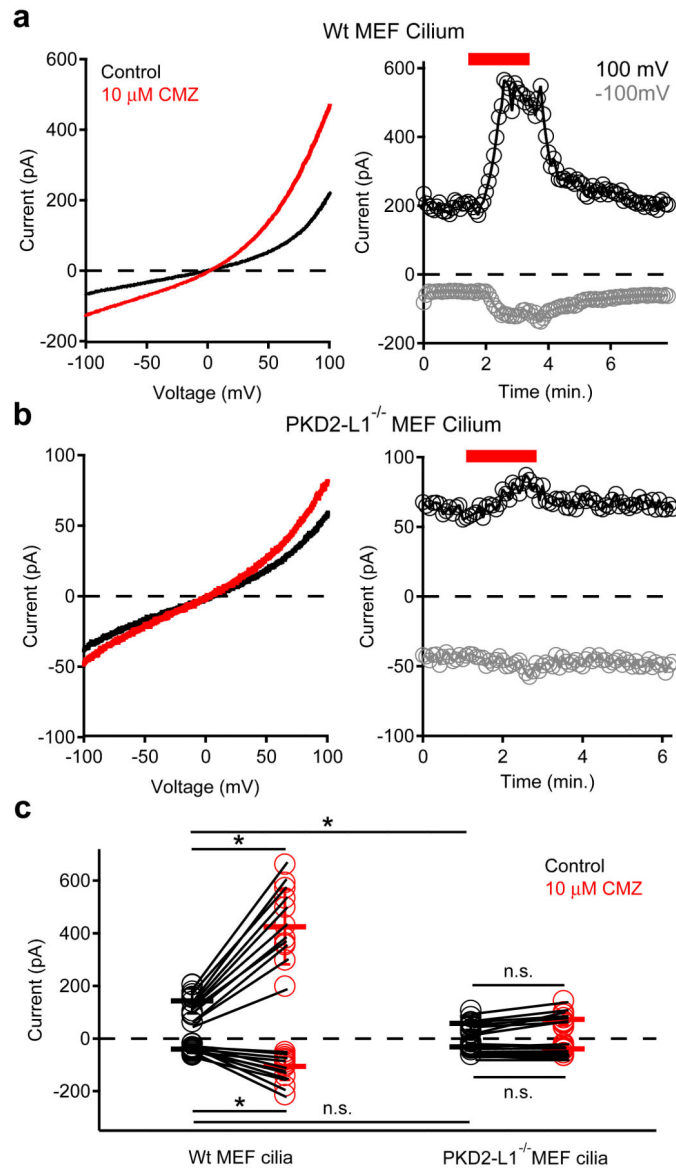


**Figure 3. MEF primary cilium currents compared from *wt* and *PKD2-L1* null animals**  
*Left*; Cilium currents recorded from MEFs isolated from (a) *wt* and (b) *PKD2-L1*<sup>-/-</sup> animals. Currents were elicited by a series of ramps from -100 to +100 mV in control conditions (black traces) or in the presence of 10  $\mu$ M calmidazolium (CMZ, red trace). *Right*; Resulting current amplitudes (-100 mV, grey circles; +100 mV, black circles) plotted as a function of time. Red bar indicates application of extracellular 10  $\mu$ M CMZ. (c) Scatter and whisker ( $\pm$  SD) plots of current magnitudes at +100 mV and -100 mV from MEF cilia. Individual cilia are represented as connected circles in control (black) and after calmidazolium (red). Averages are indicated by the dark horizontal lines. Student's t-test results: \* denotes P-value < 0.05; n.s. denotes P-value > 0.05; n = 9-11 cilia.

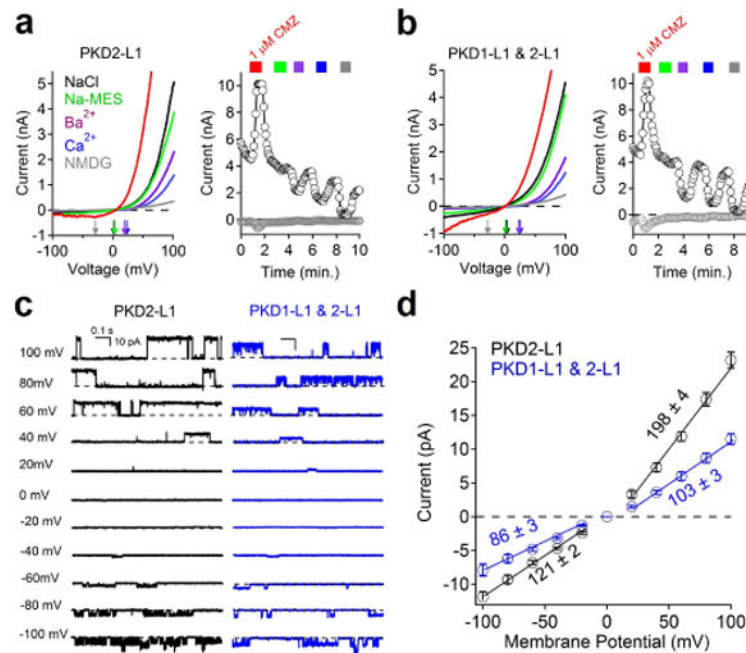
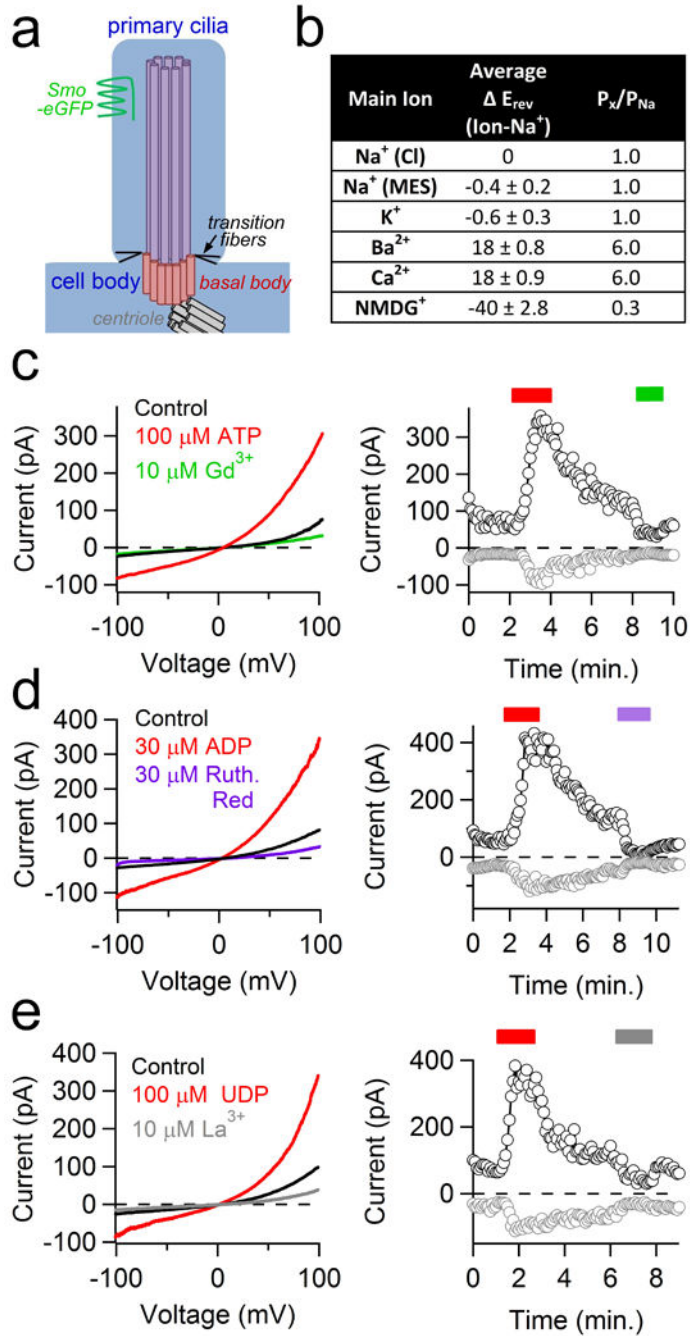


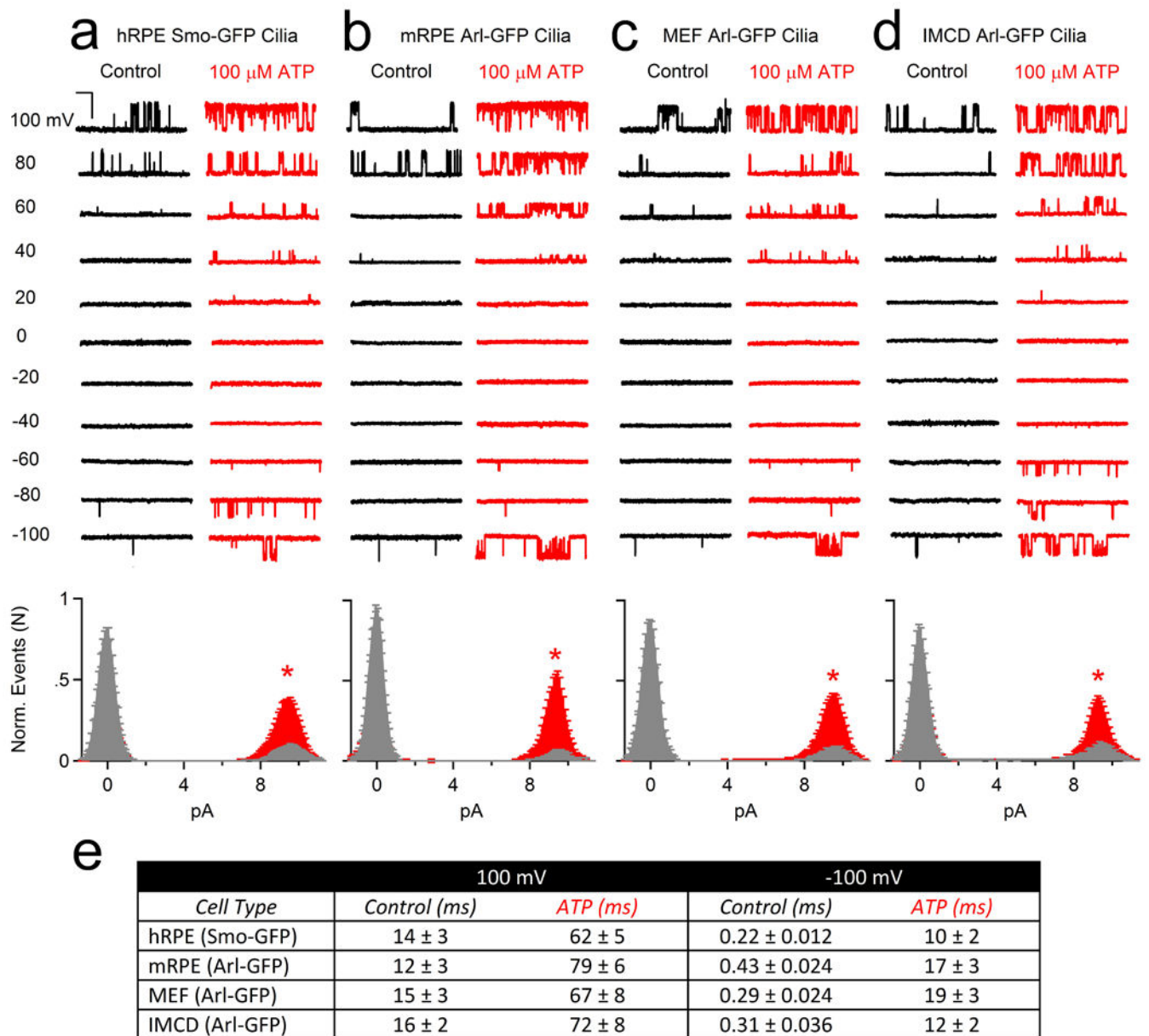
**Figure 4. Plasma membrane expressed PKD1-L1/PKD2-L1 channels match those of  $I_{cilia}$**   
**(a, b)** Whole-cell currents recorded from cells transfected with **(a)** PKD2-L1 alone or **(b)** PKD1-L1 and PKD2-L1, where extracellular 1  $\mu$ M calmidazolium (CMZ, red trace) was applied and Na<sup>+</sup>-based saline was exchanged by the cations indicated. **(c)** Single channel currents measured from the cell membrane of cells transfected by PKD2-L1 (black traces), or PKD1-L1 and PKD2-L1 (blue traces). **(d)** Resulting average single channel current amplitudes plotted against voltage measured from transfected cells ( $\pm$  SEM, n = 4-5 cells).



**Extended Data Figure 1. Ion selectivity and pharmacology of ciliary hRPE current**

(a) Diagram of the primary cilia depicting the EGFP-labeled Smoothed protein (green), transition fibers (black line), 9+0 axoneme (purple), basal body (pink) and centriole (gray). (b) Table listing the average reversal potential change relative to the standard  $\text{Na}^+$ -based extracellular solution (Average  $E_{rev}$ ) and the estimated relative permeability ( $P_x/P_{\text{Na}}$ ;  $\pm$  SEM,  $n = 4$  cilia). (c-e) *left*, Representative currents from control (black traces), activation by 100  $\mu\text{M}$  ATP, 30  $\mu\text{M}$  ADP, or 10  $\mu\text{M}$  UDP (red traces) and block by 10  $\mu\text{M}$   $\text{Gd}^{3+}$ , 30  $\mu\text{M}$  Ruthenium Red and 10  $\mu\text{M}$   $\text{La}^{3+}$  (green, violet and grey traces respectively). *Right*,

corresponding time course of peak current recorded at -100 mV (gray circles) and +100 mV (black circles).



**Extended Data Figure 2. ATP indirectly activates the cilia conductance from four different cell types**

*Top*, Single channel currents activated by 1.5 s depolarizations to the indicated potentials in control (black traces) and 100  $\mu$ M extracellular ATP (red traces) recorded from primary cilia derived from (a) human RPE Smo-GFP cell lines, (b) mouse RPE Arl-GFP primary cells, (c) mouse MEF Arl-GFP primary cells, (d) mouse kidney IMCD Arl-EGFP cells (scale = 10 pA and 200 ms). *Bottom*, corresponding open probability histograms measured in control (grey) and in the presence of 100  $\mu$ M ATP (red;  $\pm$  SEM, n = 4-6 cilia, asterisks indicates P < 0.005). (e) Average open dwell times measured from the cilia of these four cell types in control and ATP conditions.

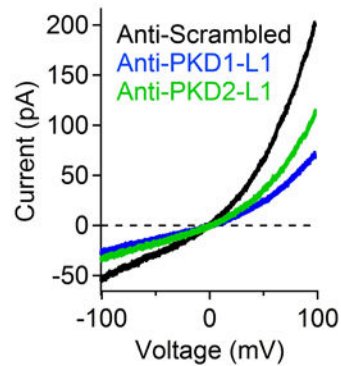
a

| Gene     | up sequence 5'-3'     | dn sequence 5'-3'      |
|----------|-----------------------|------------------------|
| hMS4A5   | CTGGGAGCAATAGCTGGAATC | CCAAAATTGAGAAAGGCAGAGA |
| hTMC7    | TCCTGTTGGTGTGTTGATCG  | TGTGACACCATGGATGAAGGA  |
| hTRPV4   | ATTATGGCTTCTCGCATACCG | GCGGCTGGACTAGAAATGAGT  |
| hPKD1-L1 | TCCTTTGGTGGTGAGCTGTC  | AGCATAGACCTCGACCCACA   |
| hPKD2-L1 | CCACCTTCACCAAGTTTGACA | GGGCTGCTCACAATAGATCG   |
| hPKD1    | CCGCTTCAAGTACGAGATCCT | CTCGGATCTTCCACACGCTAC  |
| hPKD2    | TGACTCTGAGGAGGATGACGA | TTGGCTCGCTCCATAATCTCT  |

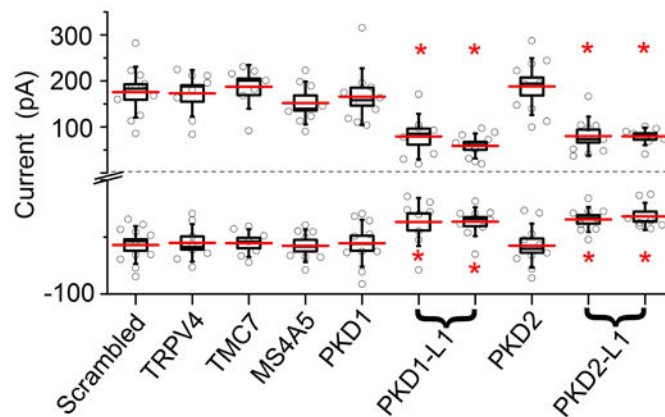
b

| siRNA against | Life technologies ID# | Knock down efficiency (SEM) |
|---------------|-----------------------|-----------------------------|
| hPKD1         | s10562                | 82 ± 4                      |
| hPKD1-L1      | s46712                | 82 ± 2                      |
| hPKD1-L1      | s46713                | 71 ± 4                      |
| hPKD2         | 104317                | 79 ± 3                      |
| hTRPV4        | s34001                | 92 ± 2                      |
| hPKD2-L1      | s17215                | 91 ± 3                      |
| hPKD2-L1      | s17216                | 95 ± 3                      |
| hMS4A5        | 130501                | 78 ± 4                      |
| hTMC7         | s33617                | 72 ± 5                      |

c



d



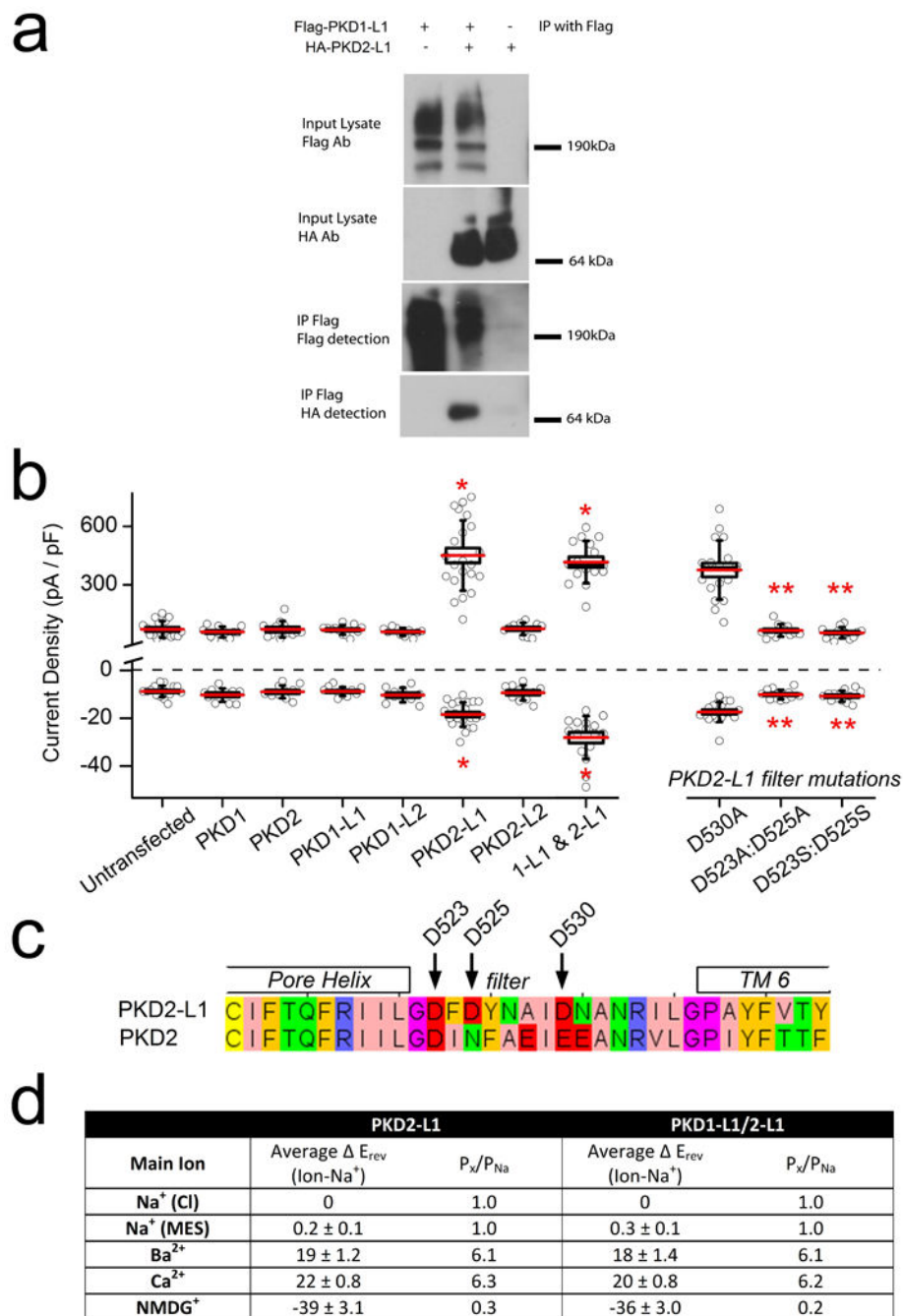
### Extended Data Figure 3. Anti-PKD1-L1 and -PKD2-L1 siRNA treatment attenuates the RPE ciliary current

(a) Table of primers used to detect transcript levels present in human RPE cells. (b) Table of siRNAs and their knockdown efficiencies used to identify channel candidates. (c) Example ciliary current measured from cells treated with siRNAs specific for PKD1-L1 or PKD2-L1.

(c) Box ( $\pm$  SEM) and whisker ( $\pm$  SD) plots of cilia total outward (+100 mV) and inward (-100 mV) current measured 72 h after double-siRNA treatment. PKD-L mRNAs were targeted by two siRNAs specific for two different regions of the target transcript. Averages



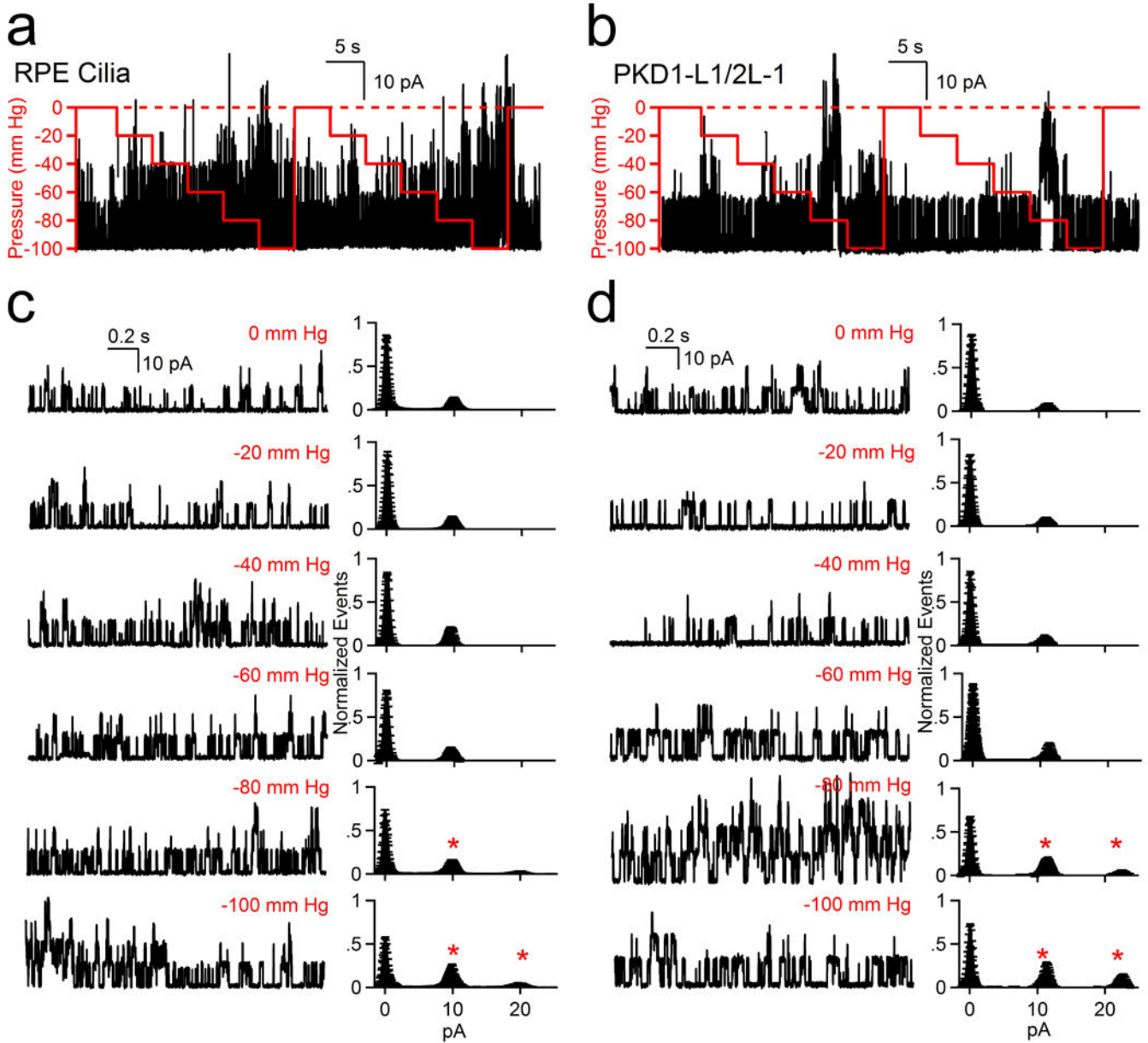
are indicated by the red lines. Student's t-test P values comparing treatment groups to scrambled siRNA: \* denotes P-value < 0.05; n = 8-12 cilia.



#### Extended Data Figure 4. Heterologous PKD1-L1 and PKD2-L1 form an ion channel

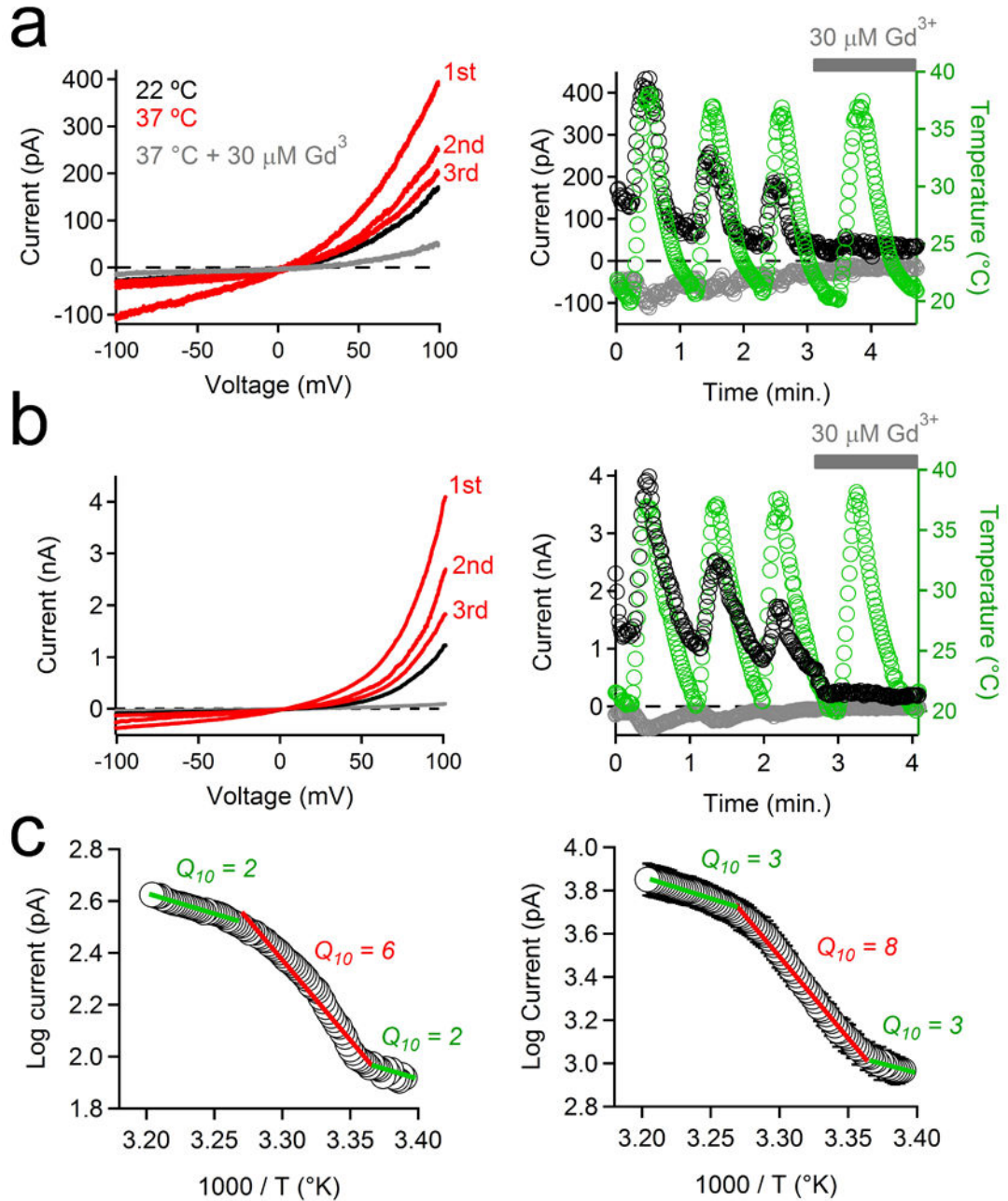
(a) Immunoprecipitation of Flag- and HA-tagged PKD1-L1 and PKD2-L1 heterologously expressed in HEK293T cells. (b) Box ( $\pm$  SEM) and whisker ( $\pm$  SD) plots of the current densities measured from PKDx-L1 family-transfected HEK cells at -100 mV (bottom) and +100 mV (top). Averages are indicated by the red lines. Statistical significance from Student's t-test comparing transfected to untransfected cells are indicated by asterisks (P-value < 0.005; n = 10-23 cells) and those comparing PKD2-L1 to the pore mutants are indicated by double asterisks (\* denotes P-value < 0.005 compared to untransfected cells; \*\*

denotes P-value < 0.005 compared to PKD 1-L1/2-L1 transfected cells; n= 9-11 cells). (c) An alignment of the PKD2-L1 and PKD2 (polycystin 2) pore helix and selectivity filter with glutamate residues D523, D525, and D530 indicated. (d) Table listing the average reversal potential change relative to the standard Na<sup>+</sup>-based extracellular solution (average  $\Delta E_{rev}$ ) and the estimated relative permeability ( $P_x/P_{Na}$ ) for HEK cells transfected with PKD2-L1 alone or with PKD2-L1 and PKD1-L1 ( $\pm$  SEM, n= 4-6 cells).



**Extended Data Figure 5. The PKD1-L1/PKD2-L1 channel is mechanosensitive only at high pressures**

(a, b) Results of pressure clamp (0-100 mm Hg, red line) on PKD1-L1/PKD2-L1 single channel events recorded from (a) RPE primary cilia and (b) HEK-293T cells transfected with PKD1-L1 and PKD2-L1. (c, d) *Left*, Expanded time scales from (a) and (b). *Right*, corresponding averaged normalized amplitude histograms are plotted for the indicated applied pipette ( $\pm$  SEM,  $n = 5$  cilia and 6 cells). Cilia or cells were held at +100 mV and pressure changes were applied at 5 s intervals. Asterisks indicate a significant ( $P > 0.05$ ) increase in channel opening events relative to the zero pressure condition.



**Extended Data Figure 6. The PKD1-L1/PKD2-L1 channel is highly temperature sensitive**  
 (a, b) The effects of repeated temperature stimulations from 22 to 37°C on the PKD1-L1/PKD2-L1 current recorded from (a) RPE primary cilia and (b) HEK-293T cells (plasma membrane) transfected with PKD1-L1 and PKD2-L1. *Left*, Currents elicited by a series of 1 Hz voltage ramps from -100 to +100 mV from 21 to 38°C in control conditions (red traces) or in the presence of 30 μM Gd<sup>3+</sup> (grey trace). *Right*, resulting current amplitudes (-100 mV, grey circles; +100 mV, black circles) and cilia temperature (green circles) are plotted as a function of time. Grey bar indicates the duration of extracellular 30 μM Gd<sup>3+</sup> application. (c) Arrhenius plots of the PKD1-L1/PKD2-L1 currents recorded from (*left*) RPE primary cilia

and (*right*) when heterologously expressed in HEK-293T cells.  $Q_{10}$  values were derived from 3 linear fits of the average normalized current magnitude from 3 phases of the thermal response (21-24°C; 24-32°C; 32-38°C;  $\pm$  SEM; n = 4 cilia or 4 cells).